Journal of Pharmaceutical and Biomedical Analysis 281 (2026) 117684

Contents lists available at ScienceDirect

Journal of Pharmaceutical and Biomedical Analysis

journal homepage: www.journals.elsevier.com/journal-of-pharmaceutical-and-biomedical-analysis

Comprehensive solution NMR characterization of bivalirudin, a direct thrombin inhibitor peptide, and its process impurities by heteronuclear spectral fingerprinting at natural isotopic abundance

Subrata H. Mishra [a,b,*,1,2], Anupreet Kaur [b], Duyen Vu [c], Sitaram Bhavaraju [c]

[a] National Institute of Standards and Technology, (formerly at US Pharmacopeial Convention, Rockville, MD, USA), Gaithersburg, MD, USA
[b] Institute for Biosciences and Biotechnology Research, University of Maryland, College Park, Rockville, MD, USA
[c] US Pharmacopeial Convention, 12601 Twinbrook Parkway, Rockville, MD, USA

ARTICLE INFO

Keywords:
Bivalirudin
[Asp^{9}]-bivalirudin
[des-Glu^{13}]-bivalirudin
Peptide impurities
NMR
Natural abundance
Structure

ABSTRACT

Bivalirudin is a 20-residue synthetic peptide that functions as a bivalent thrombin inhibitor by simultaneously engaging thrombin's active site and exosite I. Despite its widespread clinical use, comprehensive NMR-based characterization of bivalirudin and its process-related impurities has not been reported. Here, we present the first complete heteronuclear NMR analysis of bivalirudin and two major impurities—[Asp9]-bivalirudin (a deamidation-related impurity standard) and [desGlu13]-bivalirudin (a synthesis deletion)—at natural isotopic abundance. Using a combination of 1D and 2D ^{1}H, ^{13}C, and ^{15}N NMR experiments in DMSO-d_6 and aqueous solution, we achieved near-complete backbone and side-chain assignments, now deposited in the BMRB. We demonstrate that 2D heteronuclear amide maps can unambiguously differentiate the parent peptide from its process impurities. Additionally, we report the first solution-state NMR structure of free bivalirudin, revealing a compact architecture wherein the active site– and exosite-binding segments are spatially proximate, potentially reflecting a pre-binding intermediate. This study establishes a practical spectral reference framework and simplified 2D heteronuclear spectral fingerprints for structural integrity assessment and impurity tracking of bivalirudin.

1. Introduction

Bivalirudin is a synthetic 20-amino acid peptide that functions as a direct thrombin inhibitor and is used clinically to prevent blood clots [1–3]. The drug is bivalent—hence the name—engaging both the catalytic active site and exosite I [1,4] (the fibrinogen recognition site) of thrombin (Fig. 1). Structurally, bivalirudin is composed of a D-Phe--Pro-Arg-Pro tetrapeptide [5] that targets the active site, a flexible Gly$_4$ linker, and a dodecapeptide derived from residues 53–64 of the natural anticoagulant hirudin, which binds exosite I [1,4].

Due to its relatively short half-life (≈ 30 min), bivalirudin is administered via injection as a reconstituted lyophilized powder [1,3]. The chemically synthesized active pharmaceutical ingredient is manufactured using solid-phase peptide synthesis [6], which, despite advances [7,8], can introduce sequence-related impurities that may influence product quality attributes, including structural integrity, stability, and, in some cases, biological performance. Similar considerations underlie impurity control strategies for other therapeutic peptides [8], where chemically modified variants are routinely monitored as part of pharmaceutical quality assessment. Among these, [Asp^{9}]-bivalirudin, a stable impurity standard representing one of the structurally defined end products associated with deamidation of the Asn9-Gly10 region [9,10], and [des-Glu^{13}]-bivalirudin, a synthesis-related deletion [9] product missing glutamate at position 13, are two prominent and well-recognized impurities [8,11,12]. Their control is essential for pharmaceutical quality and is managed through strict manufacturing specifications and impurity thresholds (no more than criteria, 0.4% by United States Pharmacopeia [USP] monograph).

* Corresponding author at: National Institute of Standards and Technology, (formerly at U.S. Pharmacopeial Convention, Rockville, MD, USA), Gaithersburg, MD, USA.
E-mail addresses: shmishra@umd.edu, subrata.mishra@nist.gov (S.H. Mishra).
[1] Present Address: National Institute of Standards and Technology, Gaithersburg, MD, USA (formerly at U.S. Pharmacopeial Convention, Rockville, MD, USA)
[2] Present Address: Institute for Biosciences and Biotechnology Research, University of Maryland, College Park, Rockville, MD, USA

https://doi.org/10.1016/j.jpba.2026.117684
Received 28 December 2025; Received in revised form 21 July 2026; Accepted 26 July 2026
Available online 29 July 2026
0731-7085/Published by Elsevier B.V.

Chromatographic and mass spectrometric methods are routinely used to monitor peptide purity and degradation [13,14]. However, the method development and validation of these analytical methods typically involves extensive optimization, column screening, and the use of various additives in copious amounts, all of which consume significant time and resources. Nuclear magnetic resonance (NMR) spectroscopy offers an orthogonal analytical platform that complements existing methods by enabling atom-specific structural verification and impurity identification with minimal sample and solvent usage. The value of NMR identification and analysis is particularly enhanced when interrogating complex molecular structures and increasing molecular size such as the peptide materials studied and reported here.

While NMR requires an initial investment of effort to assign atom-specific chemical shifts—particularly for peptides of moderate complexity—the resulting dataset can serve as a durable reference for future lot testing, structural comparisons, and impurity profiling. Once complex 2D heteronuclear spectra are exhaustively analyzed and all signals identified, subsequent analyses of additional peptide production batches, such as in a manufacturing setting, can often rely on simpler 1D spectra (^{1}H, ^{15}N and ^{13}C), streamlining routine assessments in support of peptide synthesis and pharmaceutical quality control. Additionally, these comprehensive assignments facilitate analysis of 2D heteronuclear spectra for a specific lot, when needed, without reinvesting resources to assign spectra anew. We have previously demonstrated the utility of such 2D maps in identifying impurities, such as a single amino acid chirality change in exenatide [15], a 39-residue therapeutic peptide.

For bivalirudin, a clinically important therapeutic peptide, no such complete heteronuclear (^{1}H, ^{15}N and ^{13}C) chemical shift dataset currently exists. Its availability would enable unambiguous structural delineation and impurity tracking. Usually, the process of heteronuclear assignments would be facilitated by isotopic labeling of the relevant biomolecule. However, isotopic labeling is rarely practical in pharmaceutical settings due to cost and synthetic scale, necessitating characterization at natural isotopic abundance. While recombinant hirudin and its variants have been studied using labeled samples [16,17], these efforts have not extended to bivalirudin or its synthetic impurities in pharmaceutical formulations. Despite bivalirudin's therapeutic relevance, no comprehensive chemical shift assignments or solution-state structures of the free, unbound (to thrombin) peptide have been reported. Moreover, its known impurities, [Asp^{9}]-bivalirudin and [des--Glu^{13}]-bivalirudin, remain uncharacterized by NMR.

In the generic pharmaceutical setting, manufacturers are required to demonstrate the identity, purity, and quality of active pharmaceutical ingredients relative to recognized reference standards and pharmacopeial specifications. In the United States, the United States Pharmacopeia (USP) provides monographs and reference standards that support quality assessment in accordance with U.S. Food and Drug Administration (FDA) expectations for impurity control and pharmaceutical characterization. Consequently, the identification and characterization of known process- and degradation-related impurities constitute an important component of peptide quality assessment [11,18]. Beyond establishing the active pharmaceutical ingredient, analytical

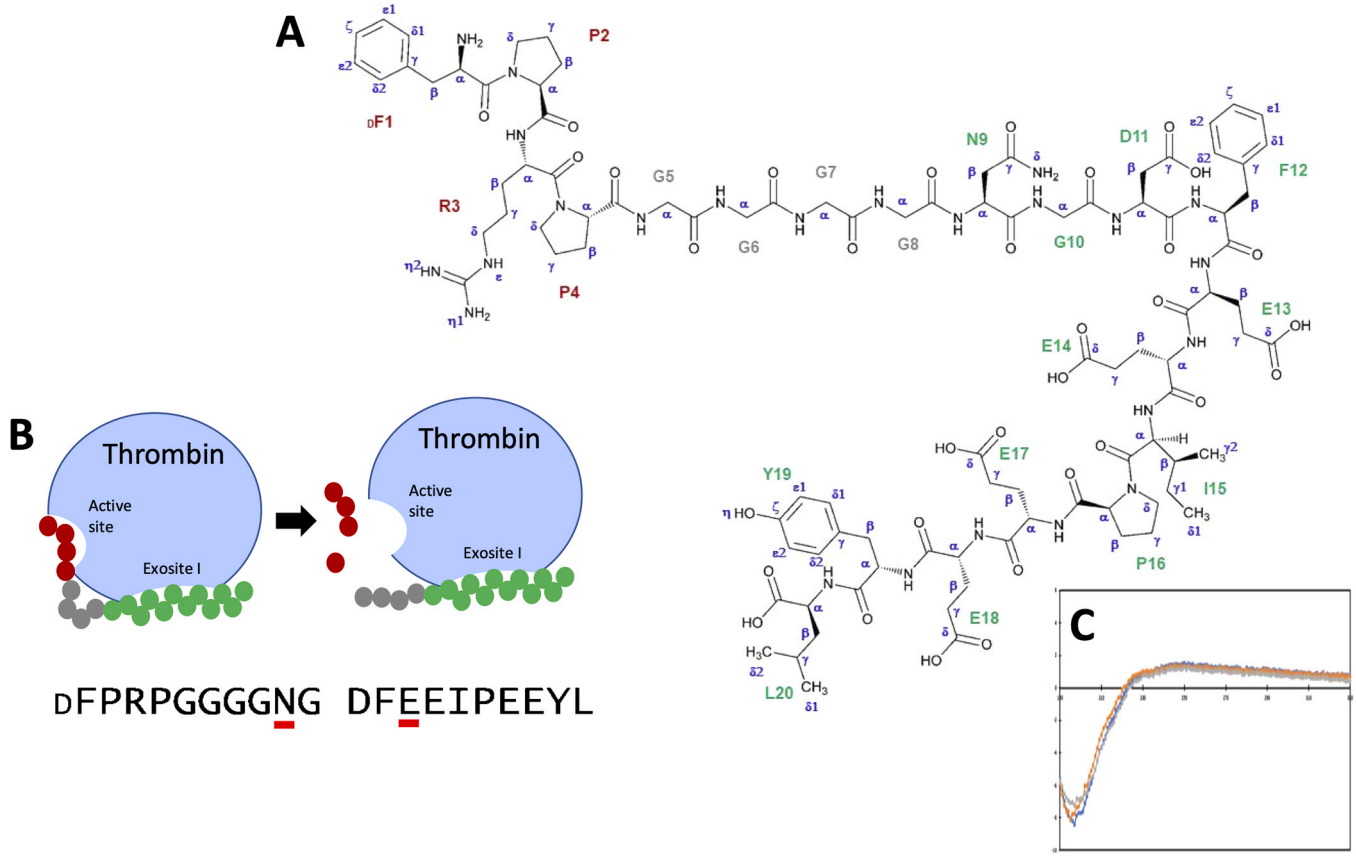

Fig. 1. Bivalirudin structure, thrombin interaction, and CD spectra comparison. (A) Chemical structure of bivalirudin annotated with amino acid positions. The only D-amino acid, the N-terminal D-phenylalanine, is indicated by $_{D}$F1. Amino acid residues are color-coded (red, gray, green) to match the peptide interacting with thrombin as illustrated in panel B. (B) Schematic representation of bivalirudin binding to thrombin (adapted from [1]), engaging both the active site and exosite I. Thrombin cleaves bivalirudin at the active site, separating the peptide into two functional segments, as previously described [1]. The peptide sequence highlights Asn9 and Glu13—residues associated with impurity variants: [Asp^{9}]-bivalirudin (deamidation mimic) and [des-Glu^{13}]-bivalirudin (synthesis impurity). (C) Overlay of CD spectra for bivalirudin, [Asp^{9}]-bivalirudin (Asn9→Asp), and [des-Glu^{13}]-bivalirudin (lacking Glu13). Spectral differences are minimal, illustrating the limited utility of CD for detecting or distinguishing such peptide variants or their mixtures.

methodologies must provide sufficient specificity to distinguish structurally related impurity species and support reference standard qualification, lot comparability, and impurity monitoring throughout manufacturing and storage.

Although deamidation of Asn-Gly motifs can generate multiple products, including Asp, succinimide intermediates, isoAsp, and D-Asp-containing species, the [Asp9]-bivalirudin standard investigated here represents a stable, structurally defined end-product arising from modification of the native N9 position. The atom-level assignments and connectivity maps reported in this study here demonstrate that deamidation-related alterations of the native peptide can be detected by NMR through comparison with structurally defined reference standards. At a minimum, comparisons to the active pharmaceutical peptide highlight deviations from the expected biopharmaceutical product. Extension of this approach through the development of additional deamidation-derived impurities reference standards would further broaden its utility for degradation monitoring.

In this study, we report the first comprehensive NMR analysis of bivalirudin and its two major impurities using natural abundance ^{1}H, ^{15}N and ^{13}C NMR spectroscopy. Assignments were performed in dimethyl sulfoxide (DMSO-d_6) for all three peptides, and additional assignments in aqueous solution were made for bivalirudin. We also present the solution-state NMR structure of bivalirudin, which provides critical insight into its unbound conformational ensemble. These NMR datasets serve as a valuable foundation for impurity identification, structural integrity assessment, and for further method development in NMR-based peptide pharmaceutical analysis.

2. Materials and methods

2.1. NMR sample preparation

All bivalirudin, [Asp^{9}]-bivalirudin, and [des-Glu^{13}]-bivalirudin peptides were obtained in lyophilized form from the United States Pharmacopeia (USP, Rockville, MD, USA) catalog. Samples were weighed and dissolved separately either in DMSO-d_6 (CIL, Andover, MA, USA) or NMR buffer - 20 mmol/L sodium phosphate, from Sigma-Aldrich (St. Louis, MO, USA), with a D_2O (CIL) volume fraction of 0.1). The aqueous buffer sodium phosphate stock had a pH of 6. The pH of the sample was checked with a microprobe and adjusted to close to 4.6 for all aqueous samples. Tetramethylsilane (TMS) and sodium 3-(trimethylsilyl) propane−1-sulfonate (DSS) (Sigma-Aldrich) were used to reference ^{1}H chemical shifts for the DMSO-d_6 and water samples respectively; ^{13}C and ^{15}N were indirectly calibrated [19]. Bivalirudin, [Asp^{9}]-bivalirudin, and [des-Glu^{13}]-bivalirudin were also orthogonally verified (data not shown) by chromatography (HPLC) and mass spectrometry (LC-MS). 13 mg to 15 mg of each peptide was dissolved in 0.7 mL for DMSO-d_6 samples. A mass of 20 mg of bivalirudin was used for the aqueous sample in NMR buffer (0.5 mL) for the heteronuclear assignments and the final NOESY spectrum used for restraint generation.

Additionally, a lower-concentration sample consisting of 5 mg of bivalirudin dissolved in NMR buffer (0.6 mL) was used to acquire NOESY spectra to assess the potential contribution of spin diffusion. The corresponding 1D ^{1}H NMR spectrum of the 5 mg sample did not display appreciable differences in linewidth or chemical shift relative to the higher-concentration sample (Supplementary Figure 5), arguing against concentration-dependent self-association as the origin of the observed long-range restraints. The pH values measured using a microprobe were 4.64 and 4.57 for the high- and low-concentration samples, respectively.

2.2. NMR data acquisition processing and analysis

All NMR data were acquired at 298 K on a commercially available Bruker (Billerica, MA, USA) Avance III 600 MHz spectrometer equipped with a room temperature triple resonance inverse (TXI) probe with a single axis gradient. All experiments were acquired with a relaxation delay of 1 s unless mentioned otherwise. Data sets were acquired and processed using the Bruker software Topspin 3.5pl6 (commercially available from the instrument manufacturer). All relevant data acquisition parameters are reported in Table 1. All data analysis and signal assignments were performed using the NMR visualization software SPARKY [20].

During processing, linear prediction was used to double the number of points in all spectra and then zero filled to 2 K points. The data were apodized in the direct and indirect dimensions using squared cosine and cosine functions respectively. The signal assignment strategy is detailed in our previous work on exenatide [15]. Chemical shifts for bivalirudin, [Asp^{9}]-bivalirudin, and [des-Glu^{13}]-bivalirudin in DMSO, and bivalirudin in water, have been deposited to the Biological Magnetic Resonance Data Bank (BMRB) database (BMRB Ids: 51621, 51622, 51623, and 51618 respectively).

The NOESY spectrum acquired with a 150 ms mixing time was used for the generation of distance restraints. To assess the potential contribution of spin diffusion to these restraints, the 5 mg sample (lower concentration) described above was used to acquire a series of NOESY spectra with mixing times of 30, 60, 90, 120, 150, and 200 ms using the same acquisition parameters listed above for the NOESY experiment, except that the spectra were acquired with a resolution of 2048 × 512 complex points (TD) and 32 scans. Cross-peak assignments were transferred to each spectrum and peak intensities were extracted using SPARKY. The intensities observed in the 200 ms spectrum were used to normalize the corresponding intensities at shorter mixing times. Analysis of representative NOE buildup curves indicated that the long-range cross-peaks used in the structure calculations were established at shorter mixing times and did not arise exclusively at the longest mixing times, where spin-diffusion effects would be expected to be most pronounced. Representative normalized NOE buildup curves for short-, medium-, and long-range contacts are shown in Supplementary Figure 6.

2.3. Structure determination using solution NMR

Bivalirudin chemical shifts were used in TALOS-N [22] for generation of dihedral restraints. Inter-proton distance restraints were derived from the NOESY spectrum and calibrated using the peak intensity of adjacent protons of an aromatic residue. Distances were binned into weak, medium, strong (5.5 Å, 4.5 Å, 3.5 Å). The distance (184) and dihedral restraints (26) were used to calculate a bundle of structures by distance geometry and simulated annealing using Xplor -NIH [23]. For

Table 1
NMR experiments[a] and relevant parameters.

Type	Spectral Width / Offset	# Points (TD) F2 x F1	Scans	Mixing Time
^{15}N HSQC	12 ppm / 4.8 ppm (^{1}H) 28 ppm / 116 ppm (^{15}N)	2048 × 128	128	-
^{15}N HSQC-TOCSY	12 ppm / 4.8 ppm (^{1}H) 24 ppm / 115.5 ppm (^{15}N)	2048 × 128	480	90 ms
^{13}C HSQC multiplicity edited	12 ppm / 4.8 ppm (^{1}H) 140 ppm / 75 ppm (^{13}C)	2048 × 128	64	-
^{13}C HSQC TOCSY	12 ppm / 4.8 ppm (^{1}H) 140 ppm / 75 ppm (^{13}C)	2048 × 512	128	90 ms
^{13}C HMBC	12 ppm / 4.8 ppm (^{1}H) 180 ppm / 95 ppm (^{13}C)	4096 × 512	480	-
^{1}H NOESY(w)	10 ppm / 4.8 ppm (^{1}H)	4096 × 512	16	150 ms

[a] Unless mentioned otherwise the same parameters (and experiments) were used for all three peptides in DMSO and for bivalirudin in water. The ^{1}H nuclear Overhauser effect spectroscopy (NOESY) spectrum was only used for water samples and is marked with (w)

the D-Phe the Xplor script was used to generate the topology file. Initially 100 structures were generated that were refined to 20, of which five were submitted as a bundle to the PDB database (https://www.rcsb.org/), chosen on the basis of geometry and minimized energy and low violations. Minimization and water solvation were performed using Xplor-NIH. These minimized structures (ensemble of 5) were deposited to the PDB database (PDB ID 8EF4). Detailed global statistics are available in the validation report of the PDB entry on the PDB database online. The corresponding PDB validation report, also available online, indicated no Ramachandran outliers within the deposited ensemble. Structure analysis and rendering of figures were performed using the program PyMOL. Lastly, the cis/trans conformations of the proline peptide bonds were evaluated using characteristic NOE patterns and established ^{13}C chemical shift criteria based on the differences between the proline C_β and C_γ chemical shifts [21].

2.4. Circular dichroism

All three peptides were compared in NMR buffer (without D_2O) via circular dichroism (CD) spectra on an Applied Photophysics Chirascan V100 spectrophotometer (Leatherhead, Surrey, UK) at 298 K. All peptides were prepared as stock solutions and evaluated (0.1 mg/mL) in a cuvette with 0.1 cm path length scanning from 180 nm to 350 nm with a step size of 1 nm and bandwidth of 1 nm. 8 scans were averaged for the final result. Data processing was done on the Chirascan Viewer, a software provided by the instrument manufacturer. The same buffer was used for blank subtraction.

3. Results and discussion

3.1. Assignment strategy

All assignments were obtained using the procedure described in our prior work on exenatide [15]. This strategy was applied to three peptides—bivalirudin, [Asp^9]-bivalirudin, and [des-Glu^{13}]-bivalirudin—in DMSO-d_6, as well as for bivalirudin in aqueous solution. Briefly, spin systems were first identified using ^{15}N and ^{13}C heteronuclear single quantum coherence–total correlation spectroscopy (HSQC-TOCSY) spectra, establishing amino acid identity. Sequence-specific connectivity was then determined using the carbonyl (C′) region (170–185ppm) of the ^{13}C heteronuclear multiple bond correlation (HMBC) spectrum, which links C_i'–HN_{i+1} pairs, where i is the residue position. These assignments were cross-validated by traditional HN–H_α correlations in the ^1H NOESY spectrum. The HMBC approach is particularly valuable in overcoming the limitations of HN–H_α nuclear Overhauser effect (NOE) patterns, which break down in the presence of proline due to the lack of an amide proton. Moreover, the HMBC spectrum provides amino acid side chain to carbonyl correlations, offering unambiguous assignment even for residues with similar carbonyl-containing sidechains. Once C′ assignments are made, 1D ^{13}C spectra can be used to monitor biophysical changes—such as binding events or conformational shifts—across the peptide backbone and carbonyl-containing side chains.

Double verification of assignments was critical given bivalirudin's challenging sequence, which includes four consecutive glycines and repeated glutamates. The ^{13}C HMBC carbonyl region enabled confident assignment by connecting the aliphatic ^1H signals of one residue to the amide and H_α signals of the next (Supplementary Figure 1). This approach is particularly advantageous for proline-containing sequences, where the amide-Hα pattern breaks down in NOESY spectra because prolines do not have amide protons. While the aliphatic region can appear crowded in the HMBC carbonyl region, the well-dispersed amide signals provide anchor points to interpret connectivity (Supplementary Figure 1).

Using this method, we obtained near-complete assignments for all three peptides in DMSO-d_6 and for bivalirudin in water. These have been deposited in the BMRB (IDs: 51621, 51622, 51623, and 51618 respectively). To our knowledge, this represents the first atomic-level NMR characterization of bivalirudin and its impurities in any solvent system. Our aim was to provide a reliable NMR-based fingerprint of bivalirudin in DMSO-d_6 to facilitate quality assessments. These assignments also enable detection of process-related impurities, such as [des-Glu^{13}]-bivalirudin (a synthesis impurity) and [Asp^9]-bivalirudin (a deamidation-related impurity), during manufacturing and storage. Additionally, shifts observed in aqueous solution can be used to track perturbations during titrations or formulation changes. Importantly, no solution structure of free bivalirudin has been reported previously. As shown later, the solution conformation of free bivalirudin and the residue-specific spectral perturbations associated with its impurity standards provide new atom-level insight into the structural consequences of sequence modification and establish a framework for future investigations of target interactions and formulation-dependent perturbations.

For consistency, atom-level assignments of bivalirudin, [Asp9]-bivalirudin, and [des-Glu13]-bivalirudin were established under identical DMSO-d_6 conditions, permitting direct comparison of their chemical-shift fingerprints and connectivity maps. From an analytical perspective, DMSO-d_6 provides a facile and reproducible environment for pharmaceutical characterization by avoiding the need for water suppression and minimizing variability arising from factors such as pH adjustment and solvent-dependent exchange effects that can complicate spectral comparisons. Consequently, these DMSO-d_6 datasets provide practical reference fingerprints that can be readily reproduced and compared against isolated impurity species and future manufacturing lots. In contrast, the aqueous NMR experiments addressed a separate objective, namely investigation of the solution conformation of free bivalirudin, for which no experimentally derived structure had previously been reported. Thus, the assignment-based pharmaceutical characterization and the aqueous structure determination represent complementary, but distinct, components of the present study.

3.2. Spectral comparison of bivalirudin and process impurities in DMSO-d_6

CD spectra of bivalirudin and its two impurities (Asp^9 and des-Glu^{13} variants) showed minimal differences (Fig. 1 C), highlighting the limitation of CD for detecting such sequence variations, even in high-purity compounds. If mixtures were present, CD may fail to provide a definitive indication of impurity.

In contrast, 2D NMR backbone amide maps clearly differentiate the peptides. Even the glycines and the glutamates in the stretch of four glycines and the two stretches of glutamates respectively have unique amide signal coordinates. These spectra, recorded in DMSO-d_6 to simplify data collection without water suppression, provide a robust comparison method even for users without extensive expertise in NMR data interpretation. For [Asp^9]-bivalirudin, the absence of the asparagine side-chain amine is evident (Fig. 2), but the most prominent differences span residues G8–E13, with significant perturbations at N9–D11. These shifts likely reflect fast-timescale dynamic changes not captured by CD, yet provide diagnostic markers in both 2D and even 1D ^1H spectra—particularly for the shifted N9 signal, which is well-resolved. Notably, the chemical distinction between bivalirudin and [Asp^9]-bivalirudin is minimal—only the loss of a side-chain amine; yet their respective NMR 2D ^{15}N heteronuclear maps provide distinct fingerprints. This reinforces the diagnostic capability of 2D heteronuclear NMR, consistent with prior observations on exenatide, where a change in chirality at a single residue yielded similar spectral discrimination [15].

For [des-Glu^{13}]-bivalirudin, the largest perturbations occur at E14 and I15 (with E13 absent). Although the amide ^1H shifts—if evaluated alone—may obscure these changes, the loss of E13 and movement of I15 should still remain discernible in the amide proton spectrum. Obviously

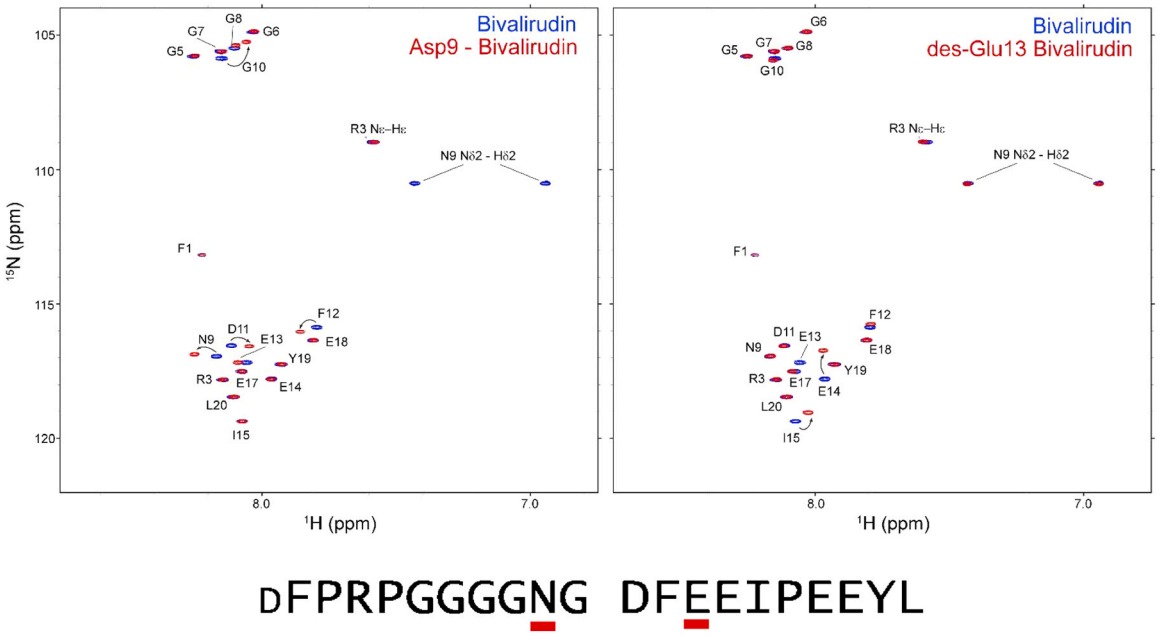

Fig. 2. 2D ^{15}N heteronuclear maps of bivalirudin and process impurities in DMSO. ^{15}N HSQC spectral overlays of bivalirudin with [Asp^{9}]-bivalirudin and [des-Glu^{13}]-bivalirudin shows clear differences at the level of the amide bond which will be beneficial when drug substance is present with impurities. All three spectra are for samples in DMSO-d_6. The arginine side chain is folded into the spectra to preserve resolution. The arrows indicate the corresponding signal for the same amide in the bivalirudin impurities. The stark differences facilitate visual analysis of the spectra. The ^{13}C spectrum encompassing the Cα backbone atoms are also compared in supporting information (Supplementary Figure 2) but they do not show the stark differences observed in the backbone amide spectra (^{15}N-HSQC).

acquiring 2D ^{15}N heteronuclear spectral maps (at natural abundance) will provide unambiguous identification, even in mixtures.

Complementary 2D ^{13}C HSQC spectra targeting C_α resonances also reveal distinctions (Supplementary Figure 2). However, unlike amide maps, these differences are more localized—primarily at N9 (Asp^{9} variant) and E13 (des-Glu^{13} variant). Beyond 2D comparisons, 1D ^{13}C spectra spanning the aliphatic to carbonyl regions can now be interpreted with confidence due to the deposited assignments. Likewise, the 1D trace of a ^{15}N HSQC (first increment of a 2D ^{15}N HSQC spectrum) isolates backbone amides from aromatic and side-chain protons, further aiding rapid comparison. Taken together, these datasets enable efficient impurity detection and characterization using simplified spectral readouts.

An important distinction exists between pharmaceutical characterization and traditional biomolecular structure determination. In structural biology, resonance assignments are often viewed primarily as an intermediate step toward high-resolution structure determination. In pharmaceutical characterization, however, atom-level assignments and connectivity relationships are themselves a characterization endpoint because they provide direct experimental evidence of molecular identity that is transferable, verifiable, and readily compared across laboratories, manufacturing lots, and reference materials. Thus, heteronuclear chemical shifts, together with multidimensional connectivity information, serve as analytical fingerprints that enable unambiguous and facilitated identification of active pharmaceutical ingredients and related impurity species. Once such assignments have been established, subsequent analyses can often rely on simplified spectral comparisons without reinvesting resources in complete reassignment.

Building on these spectral distinctions, we observe from Fig. 2 that—apart from the missing NH_2 side-chain resonances—a few isolated signals remain unchanged between bivalirudin and [Asp^{9}]-bivalirudin. This provides a framework to quantitatively monitor deamidation of bivalirudin over time. Identifying which signals shift (i.e., show different chemical shifts between bivalirudin and [Asp^{9}]-bivalirudin) allows strategies that use intensity ratios between signals expected to move or disappear (N9 amino groups) and those that remain stable to quantify deamidation. For example, monitoring the intensity (I) of selected peaks over time —signal Y19 (either one or both peaks of the doublet, marked as I_1), the rightmost component of the triplet encompassing amide signals F12 and E18 (I_2), and one or both amino signals (I_3) and comparing the ratios I_3/I_1 and I_2/I_1 (Supplementary Figure 3 A) allows one to track deamidation. Both ratios are expected to decrease with increase in deamidation and thus provide a quantitative means to follow this change. The lowest detectable percentage of deamidation will depend on the signal-to-noise ratio (S/N) of the peaks involved; for example, detecting 1% deamidation with statistical confidence requires that the S/N exceeds a defined threshold.

Similarly, to detect [des-Glu^{13}]-bivalirudin as an impurity, we can analyze the central peaks of the triplets corresponding to G5 (I_1), G6 (I_2), and F12 + E18 (I_3) in the 1D spectra (Supplementary Figure 3B). As evident from the 2D maps in Fig. 2 and the 1D overlays of [des-Glu^{13}]-bivalirudin and bivalirudin in Supplementary Figure 3B, these signals retain their positions and intensities for I_1 & I_3, but their intensities vary for I_2 between the two peptides. For I_2 this occurs because the amide signal for I15 coincides with G6 in [des-Glu^{13}]-bivalirudin. For bivalirudin, the ratios I_2/I_1 and I_2/I_3 are 1.1 and 0.7, respectively; for des-Glu13, the corresponding ratios are 1.6 and 1 (Supplementary Figure 3B). These distinct values indicate that, if 1D ^{1}H spectra of bivalirudin are acquired with sufficient S/N, even low levels of des-Glu^{13} impurities can be quantified, provided the remaining spectral profile resembles that of bivalirudin. While these ratio ranges require further validation across experimental conditions, the present study establishes a foundation for such quantitative impurity analyses.

3.3. *Assignments and structure of bivalirudin in aqueous solution*

We also performed near-complete assignments of bivalirudin in aqueous solution (BMRB ID: 51618). The same strategy used in DMSO-*d6*, and previously applied to exenatide, enabled unambiguous identification of backbone amide and C_α resonances (Fig. 3B, C) along with carbonyl and side-chain resonances. These assignments (aqueous) are valuable for future studies using labeled protein targets (e.g., ^{13}C,^{15}N-

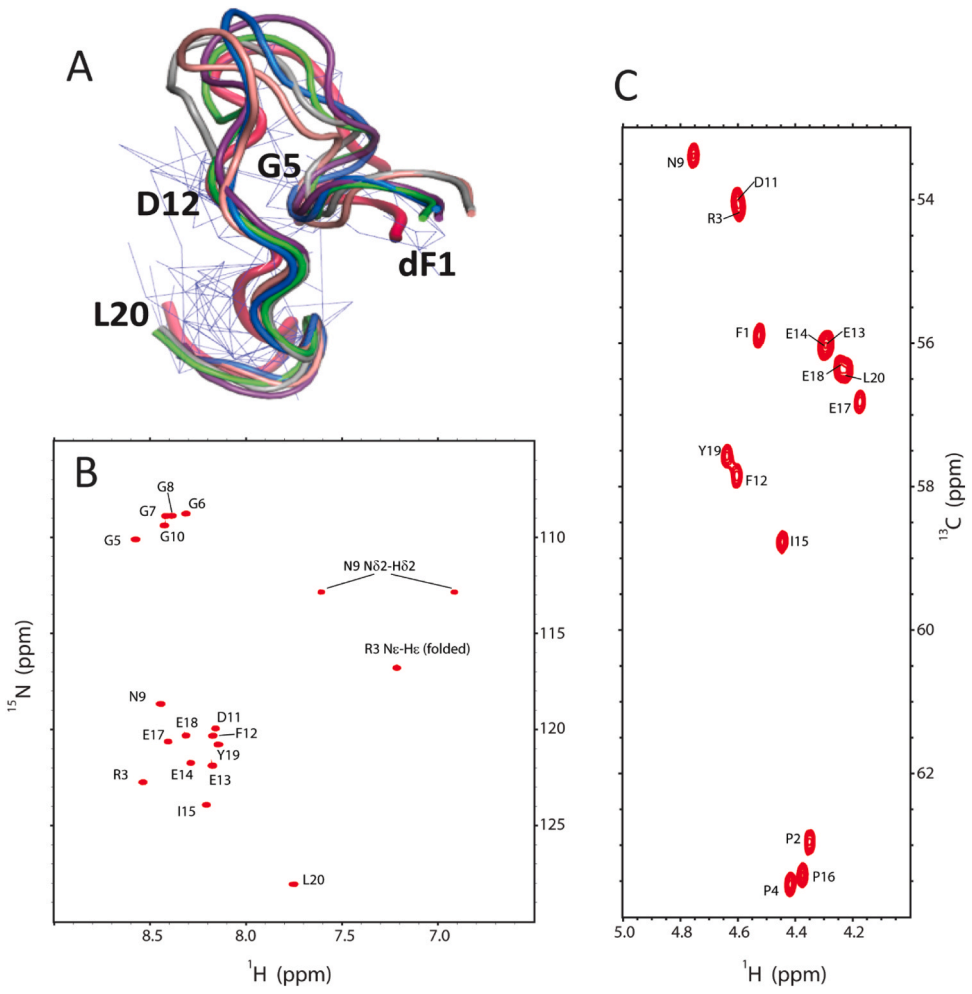

Fig. 3. NMR solution structure of bivalirudin and backbone fingerprint maps under aqueous conditions. (A) Backbone-only structure of bivalirudin calculated from NOESY-derived distance restraints (red) acquired in aqueous solution. An ensemble of five low-energy conformers that satisfy all experimental restraints is shown, with select residue positions labeled. (B) Assigned ^{15}N HSQC spectrum of bivalirudin in water. (C) Assigned ^{13}C HSQC spectrum (C_α region) of bivalirudin in water.

thrombin), where NOE-based experiments can isolate bivalirudin atoms interacting with the target or subject to conformational rearrangement due to the interaction. For instance, atomic-level interactions between a ^{13}C ^{15}N labeled thrombin and an unlabeled bivalirudin molecule can be identified using a NOESY experiment that is doubly-edited (^{13}C ^{15}N) in one dimension to select cross peaks from amide protons attached to a ^{13}C atom (C' or C_a) and singly edited (^{15}N only) in the second dimension to select amide protons attached to a ^{12}C atom.

The cis/trans conformations of the three proline peptide bonds were evaluated using characteristic NOE patterns together with established ^{13}C chemical shift criteria based on the differences between the proline C_β and C_γ chemical shifts [21]. Both approaches were consistent with predominantly trans peptide bond conformations for all three proline residues in bivalirudin. Furthermore, even in the higher-concentration sample NOESY spectrum, no minor cross-peaks indicative of an alternative cis-proline population were observed. These observations suggest that any cis conformers, if present, were below the level of detection under the experimental conditions employed.

This dataset fills a significant gap—prior to this study, no NMR solution structure of free bivalirudin has been reported. Existing crystal structures [24] depict only its split tetrapeptide and dodecapeptide segments bound to thrombin's active catalytic site and exosite I (Supplementary Figure 4). A complete structure may have been elusive due to conformational flexibility. Using ^{1}H NOESY-derived distances and dihedral angles from heteronuclear chemical shifts, we generated an ensemble of five structures (PDB ID: 8EF4) (Fig. 3A). The bivalent segments of bivalirudin independently adopt consistent conformations within the ensemble while the glycine linker fans out. Limited NOEs were found in the flexible glycine-rich linker; however, NOESY distance restraints between the tetrapeptide (D-Phe-Pro-Arg-Pro) segment and the hirudin-analog region constrain it to fold back. The bivalent segments do not display elements that allow categorization to standard secondary structure elements like the α helix or 3_{10} helix evidenced from the backbone dihedral angles and have a coil like architecture. This architecture is also reflected in the lower dispersion of the amide protons in the ^{15}N HSQC spectrum.

This folded arrangement of the bivalent segments of bivalirudin may reflect a functional intermediate important for thrombin binding. Binding is expected to involve a conformational transition from the folded state (as in our solution ensemble) to an extended bound state (per crystal structures) [24]. Deamidation-related modification at the N9 position introduces a local change in charge that could influence this conformational equilibrium, although the functional consequences of such perturbations remain to be determined.

4. Conclusions

We previously demonstrated the utility of simplified 2D heteronuclear amide maps acquired by NMR at natural abundance in distinguishing peptide variants of exenatide, where a single chirality

change was detectable [15]. Here, we extend this approach to bivalirudin and its process-related impurities, showing that even subtle sequence variations (e.g., loss of a side-chain or residue) produce distinct spectral fingerprints.

We carried out comprehensive heteronuclear assignments in both DMSO-d_6 and aqueous environments, and deposited them to the BMRB to support future studies. These 2D NMR maps, which track the peptide amide backbone, provide a means to distinguish variants (desired drug substance *vs.* the deamidated or deleted versions), which CD spectroscopy is unable to provide. The distinct changes observed by NMR likely arise from changes in fast-timescale regime and local environment changes, making it a high-information content tool for structural quality assessment of biotherapeutic peptides. In pharmaceutical characterization, atom-level assignments and connectivity relationships are not merely a preliminary step toward structure determination; they constitute transferable analytical fingerprints that enable impurity identification and comparison across reference standards and manufacturing lots. Consistency between reference and experimental chemical shifts confirms the structural integrity of the active pharmaceutical ingredient, whereas deviations in peak position, intensity indicate impurity formation, degradation, or other structural perturbations requiring further evaluation. Thus, NMR chemical shifts provide a direct link between atom-level structural characterization and pharmaceutical quality control. While further studies are needed to probe the dynamic regimes underlying these chemical shift changes, our datasets enable practical workflows for impurity detection. We presented the first NMR-based solution structure of free bivalirudin, shedding light on a potential relationship between conformational states and function.

In summary, this study delivers a robust atomic-level framework for characterizing bivalirudin and its impurities, facilitating pharmaceutical quality control, through transferable atom-level fingerprints for impurity identification and orthogonal quality assessment of generic peptide therapeutics [25].

CRediT authorship contribution statement

Sitaram Bhavaraju: Writing – review & editing, Validation, Resources, Project administration. **Duyen Vu:** Investigation, Data curation. **Anupreet Kaur:** Writing – review & editing, Investigation, Data curation. **Subrata H. Mishra:** Writing – review & editing, Writing – original draft, Visualization, Investigation, Formal analysis, Data curation.

Role of the funding sources

This research did not receive any specific grant from funding agencies in the public, commercial, or not-for-profit sectors.

Disclaimer

Certain commercial equipment, instruments, vendors, materials, and software may be identified in this manuscript to specify adequately the experimental procedure(s). Such identification does not imply approval, endorsement, or certification of a particular brand or product, nor does it imply that the equipment, instrument, vendor, or material is necessarily the best available for the purpose or that any other brand or product was judged to be unsatisfactory or inadequate.

Declaration of Competing Interest

The authors declare that they have no known competing financial interests or personal relationships that could have appeared to influence the work reported in this paper.

Acknowledgments

The authors would like to acknowledge and thank the internal scientific reviewers at USP and the National Institute of Standards and Technology for their constructive comments and to Charles Schwieters (NIH, NIDDK) for help with the Xplor-NIH software.

Appendix A. Supporting information

Supplementary data associated with this article can be found in the online version at doi:10.1016/j.jpba.2026.117684.

References

[1] T.E. Warkentin, A. Koster, Bivalirudin: a review, Expert. Opin. Pharmacother. 6 (8) (2005) 1349–1371, https://doi.org/10.1517/14656566.6.8.1349.
[2] C.J. Lee, J.E. Ansell, Direct thrombin inhibitors, Br. J. Clin. Pharmacol. 72 (4) (2011) 581–592, https://doi.org/10.1111/j.1365-2125.2011.03916.x.
[3] H. Mccarthy, C. Dyke, Use of bivalirudin as an anticoagulant during cardiopulmonary bypass health disparities in minority populations; management of bleeding and thrombosis after surgery, J. Extra Corpor. Technol. 37 (3) (2005) 296–302.
[4] T.E. Warkentin, Bivalent direct thrombin inhibitors: hirudin and bivalirudin, Best. Pract. Res. Clin. Haematol. 17 (1) (2004) 105–125, https://doi.org/10.1016/j.beha.2004.02.002.
[5] Z. Su, A. Vinogradova, A. Koutychenko, D. Tolkatchev, F. Ni, Rational design and selection of bivalent peptide ligands of thrombin incorporating P4-P1 tetrapeptide sequences: From good substrates to potent inhibitors, Protein Eng. Des. Sel. 17 (8) (2004) 647–657, https://doi.org/10.1093/protein/gzh073.
[6] J.M. Maraganore, P. Bourdon, J. Jablonski, K.L. Ramachandran, J.W. Fenton, Design and characterization of hirulogs: a novel class of bivalent peptide inhibitors of thrombin, Biochemistry 29 (30) (1990) 7095–7101, https://doi.org/10.1021/bi00482a02.
[7] A.S. Droz, J. Schnidrig, N. Studer, S. Varray, C. Wenger, O. Werbitzky, Method for solid phase peptide synthesis, US Pat. USRE46830E1 (2005).
[8] G. Krishna, G. Musso, Pharmaceutical formulations of bivalirudin and processes of making the same, US Pat. US7582727B1 (2008).
[9] M. D'Hondt, N. Bracke, L. Taevernier, B. Gevaert B, F. Verbeke, E. Wynendaele, B. De Spiegeleer, Related impurities in peptide medicines, J. Pharm. Biomed. Anal. 101 (2014) 2–30, https://doi.org/10.1016/j.jpba.2014.06.012.
[10] K. Kato, T. Nakayoshi, E. Kurimoto, A. Oda, Mechanisms of deamidation of asparagine residues and effects of main-chain conformation on activation energy, Int. J. Mol. Sci. 21 (19) (2020) 1–14, https://doi.org/10.3390/ijms21197035.
[11] D. McCarthy D, Y. Han, K. Carrick, D. Schmidt, W. Workman, P. Matejtschuk, C. Duru, F. Atouf, Reference standards to support quality of synthetic peptide therapeutics, Pharm. Res. 40 (6) (2023) 1317–1328, https://doi.org/10.1007/s11095-023-03493-1.
[12] A. Tovi, C. Eidelman, S. Shushan, A. Hagi, A. Ivchenko, G.-M. Butilca, L. Bar-Oz, T. Gadi, G. Zaoviå, Process for production of bivalirudin, US Pat. US20130196919A1 (2006).
[13] K. Zeng, I. Geerlof-Vidavisky, A. Gucinski, X. Jiang, M.T. Boyne, Liquid chromatography-high resolution mass spectrometry for peptide drug quality control, AAPS J. 17 (3) (2015) 643–651, https://doi.org/10.1208/s12248-015-9730-z.
[14] K.Y.K. Kumar, V.R. Dama, C. Suchitra, T.C. Maringanti, A simple, sensitive, high-resolution, customized, reverse phase ultra-high performance liquid chromatographic method for related substances of a therapeutic peptide (bivalirudin trifluoroacetate) using the quality by design approach, Anal. Methods 12 (3) (2020) 304–316, https://doi.org/10.1039/c9ay01998g.
[15] S.H. Mishra, S. Bhavaraju, D.R. Schmidt, K.L. Carrick, Facilitated structure verification of the biopharmaceutical peptide exenatide by 2D heteronuclear NMR maps, J. Pharm. Biomed. Anal. 203 (2021) 114136, https://doi.org/10.1016/j.jpba.2021.114136.
[16] X. Song, W. Mo, X. Liu, L. Zhu, X. Yan, H. Song, L. Dai, The NMR solution structure of recombinant RGD-hirudin, Biochem. Biophys. Res. Commun. 360 (1) (2007) 103–108, https://doi.org/10.1016/j.bbrc.2007.06.014.
[17] Y. Huang, Y. Zhang, Y. Wu, J. Wang, X. Liu, L. Dai, L. Wang, M. Yu, W. Mo, Expression, purification, and mass spectrometric analysis of ^{15}N, ^{13}C-labeled RGD-hirudin, expressed in Pichia pastoris, for NMR studies, PLoS. One 7 (8) (2012) e42207, https://doi.org/10.1371/journal.pone.0042207.
[18] U.S. Department of Health and Human Services, Food and Drug Administration, Center for Drug Evaluation and Research (CDER). ANDAs for certain highly purified synthetic peptide drug products that refer to listed drugs of rDNA origin; guidance for industry. May 2021 (accessed June 2026). http://resource.nlm.nih.gov/9918350982606676.
[19] R.K. Harris, E.D. Becker, S.M.C. De Menezes, P. Granger, R.E. Hoffman, K.W. Zilm, Further conventions for NMR shielding and chemical shifts (IUPAC recommendations 2008), Magn. Reson. Chem. 46 (6) (2008) 582–598, https://doi.org/10.1002/mrc.2225.
[20] W. Lee, M. Tonelli, J.L. Markley, NMRFAM-SPARKY: enhanced software for biomolecular NMR spectroscopy, Bioinformatics 31 (8) (2015) 1325–1327, https://doi.org/10.1093/bioinformatics/btu830.

[21] M. Schubert, D. Labudde, H. Oschkinat, P. Schmieder, A software tool for the prediction of Xaa-Pro peptide bond conformations in proteins based on 13C chemical shift statistics, J. Biomol. NMR 24 (2002) 149–154, https://doi.org/10.1023/A:1021613726416.
[22] Y. Shen, A. Bax, Protein backbone and sidechain torsion angles predicted from NMR chemical shifts using artificial neural networks, J. Biomol. NMR 56 (3) (2013) 227–241, https://doi.org/10.1007/s10858-013-9741-y.
[23] C.D. Schwieters, J.J. Kuszewski, N. Tjandra, G. Marius Clore, The Xplor-NIH NMR molecular structure determination package, J. Magn. Reson. 160 (1) (2003) 65–73, https://doi.org/10.1016/S1090-7807(02)00014-9.
[24] T. Yamada, K. Kurihara, Y. Ohnishi, T. Tamada, K. Tomoyori, K. Masumi, I. Tanaka, R. Kuroki, N. Niimura, Neutron and X-ray crystallographic analysis of the human α-thrombin-bivalirudin complex at pD 5.0: protonation states and hydration structure of the enzyme-product complex. Biochim. Biophys. Acta 1834 (8) (2013) 1532–1538, https://doi.org/10.1016/j.bbapap.2013.05.014.
[25] O. Zupančič, J.A. Grießinger, H.T. Lam, A. Bernkop-Schnürch, Storage stability of bivalirudin: hydrophilic versus lipophilic solutions, J. Pharm. Sci. 106 (5) (2017) 1322–1330, https://doi.org/10.1016/j.xphs.2017.01.019.